UNIVERSIDADE DE SÃO PAULO

INSTITUTO DE FÍSICA
CAIXA POSTAL 20516
01498 SÃO PAULO - SP
BRASIL

PUBLICAÇÕES

IFUSP/P-975

TRANSPORT IN THE PLASMA EDGE OF A TOKAMAK WITH HIGH MHD ACTIVITY

Raul M. Castro, Maria Vittória A.P. Heller, Iberê L. Caldas, Ruy P. da Silva, Zoezer A. Brasilio, TBR-I Team
Instituto de Física, Universidade de São Paulo

Março/1992

TRANSPORT IN THE PLASMA EDGE OF A TOKAMAK WITH HIGH MHD ACTIVITY

Raul M. Castro, Maria Vittória A.P. Heller, Iberê L. Caldas,

Ruy P. da Silva, Zoezer A. Brasilio, TBR–I Team

Institute of Physics, University of São Paulo
C.P. 20516, 01498 – São Paulo, S.P., Brazil

ABSTRACT

Electrostatic turbulence and various aspects of magnetic fluctuations have been investigated, in the edge region of the TBR–1 Tokamak, by using a set of Langmuir and magnetic probes, and a triple probe. Measurements of plasma parameters such as potential, density, temperature and magnetic field were taken in order to elucidate the effect on transport of the electrostatic and magnetic fluctuations in the edge. The fluctuations levels are found to be higher than in most tokamak discharges. The particle flux is outward and of the order of that calculated from Bohm diffusion, and occurs in the frequency region typical of the macroscopic MHD oscillations. The Mirnov oscillation frequencies in TBR–1 are higher than those observed in other tokamaks and, consequently, there is an uncommon superposition between the Mirnov and turbulent density fluctuations spectra. This fact and the presence of high MHD activity may contribute to elucidate possible influence of the magnetic oscillations on the electrostatic transport observed in plasma edge.

I. INTRODUCTION

Energy and particle transport in tokamaks are much higher than predicted from neoclassical theory, and there are experimental evidences that they are associated to the presence of plasma turbulence (Wootton, 1990). Much work has been done to understand the basic mechanisms of this anomalous transport and to determine whether it can be explained by either electrostatic or magnetic fluctuations (Diamond et al., 1990).

Research on basic experiments in tokamaks plays an important role in developing the understanding of transport in these devices. Thus, analyses of fluctuation spectra, an example of this effort, try to identify the relevant transport phenomena and to test current theoretical models. These analyses are performed with data obtained from diagnostics that measure broadband fluctuations in the inner part of the plasma, and measurements with Langmuir and magnetic probes located at the plasma edge (Kim et al., 1991). These measurements provide information about the influence of the plasma edge turbulence on plasma confinement, a relevant subject after the discovery of L and H confinement modes in ASDEX (Wagner et al., 1982).

Characteristics of broadband fluctuations related to the phenomena of transport have been obtained by knowing their statistical dispersion relations (Wootton, 1990). These dispersion relations have been experimentally determined by using correlation techniques to analyse signals which are measured at different spatial locations (Ritz et al., 1984). Detailed measurements carried out in tokamaks and other machines have shown that broadband electrostatic fluctuations are large enough to explain anomalous transport in plasma edge (Ritz et al., 1989; Hidalgo et al., 1991; Robinson, 1986). On the other hand, although the magnetic fluctuations are usually not directly significant for transport, they are a useful indication of edge turbulence (Kim et al., 1991). While the major part of this progress was made on conventional tokamaks, experiments with tokamak discharges with high MHD activity and turbulence, like those reported in this article, may contribute

to emphasize relevant aspects not observed in other devices.

Although magnetic fluctuations have been associated with discharge quality and confinement degradation (Wootton, 1990), experimental limitations have made it difficult to prove causal relations. In TEXT, correlations between a magnetic probe measuring magnetic fluctuation and a Langmuir probe measuring density fluctuation have shown that the coherency between these fluctuations is strong and significant only at high frequency, the range that accounts for most of the transport associated with the density turbulence, and only when the Langmuir probe is inside the limiter radius (Kim et al., 1991; Tsui et al., 1991). Although there were strong fluctuations in both density and magnetic field, the dominant part of the magnetic and density fluctuation frequency spectra were well separated and furthermore the Mirnov oscillations (low–m number modes) frequencies were much lower than the average density fluctuation frequency. It was also observed that plasma edge conditions were significantly altered during high MHD discharges or modified by externally applied helical magnetic field (Tsui et al., 1991; Roberts et al., 1991; Lippman et al., 1991; Ribeiro et al., 1990), as it was suggested in (Karger and Lackner, 1977). Therefore, there are clear evidences that the magnetic fluctuation does not contribute directly to the fluctuation–driven particle flux but, on the other hand, the possibility that it might influence the particle transport indirectly via a non–linear coupling with the electrostatic fluctuation cannot yet be ruled out.

As it is reported in this paper, in the TBR–1 tokamak, near the limiter, the Mirnov oscillations and the dominant part of the density (and floating potential) fluctuation power spectra have similar frequencies and most of the transport associated with the electrostatic turbulence occurs in this frequency range. This fact may give new information about the possible influence of the magnetic oscillations on the electrostatic transport in the tokamak plasma edge.

The objective of the present investigation is to characterize the local, statistical space/time propertiees of the turbulence observed in the plasma edge of the TBR–1, a

small tokamak with high MHD activity and turbulence, and to estimate directly the effect of the turbulence on particle transport. The edge potential and density fluctuations were measured with Langmuir probes and the edge magnetic fluctuations with magnetic probes. Estimations of wavenumber frequency spectra $S(k,\omega)$ of these fluctuations were based on a two–point correlation technique and the fluctuation–induced particle transport is determined by a method that have been applied to analyse fluctuations in the TEXT tokamak (Levinson et al., 1984). In addition, the density, floating potential, and electron temperature radial profiles were also measured and their gradients and length scales were determined to discern instabilities which may be responsible for the turbulence. The experimental details are given in Section 2. Equilibrium and fluctuations profiles, fluctuations spectra, correlations and transport are presented in Section 3. Discussions of the results and conclusions are given in Section 4.

2. EXPERIMENTAL SET–UP AND MEASUREMENTS

TBR–1 is a small ohmically heated tokamak (minor radius a = 8 cm, major radius R = 30 cm). For the reported experiments the machine was operated with a central electron temperature $T_e(o) \cong 2 \times 10^2$ eV, central density $n(o) \cong 6 \times 10^{12}$ cm^{-3}, plasma current $I_p \cong 8.5$ kA, toroidal field $B_\phi = 0.4$ T (corresponding to a safety factor $q(a) \cong 5$).

A square array of four single Langmuir probes, separated both toroidally and poloidally by 2 mm, was located at the top of the tokamak along the plasma centerline and it was used to measure density and potential fluctuations. The electron temperature and density profiles were measured with a triple probe (Chen and Sekiguchi, 1965). In the present analysis the effect of temperature fluctuations on the interpretation of saturation current fluctuations in terms of density fluctuations is neglected. The poloidal and the radial components of magnetic oscillations were measured near Langmuir probes by a set of

four radially separated coils, two of these coils measured poloidal components and the other two coils radial components. This experimental set–up is similar to another one used in the TEXT tokamak (Hollenstein et al., 1986; Duperrex, 1984). The signals were digitized at 1 MHz, using a 8 bit digitizer. Digital spectral analysis based on a correlation technique developed by Powers and collaborators (Powers, 1990) were used to reduce the information contained in the time series of $\tilde{n}(t)$, $\tilde{\varphi}(t)$, $\dot{\tilde{B}}_\theta(t)$ and $\dot{\tilde{B}}_r(t)$ obtained from the probes. The data presented (averaged over four consecutive shots) were obtained during intervals of approximately 2.0 ms, averaged after the plasma current reaches an appropriate plateau.

Data from the four–probe array were collected and the electron density and floating potential profiles were estimated and their amplitudes used in the numerical analysis of Section 3.

Measurements were made in the region accessible to the probes, i.e., $r/a \cong 0.80 - 1.25$. Temperature time averaged measurements from the triple proble are shown in Fig. 1; there, the error bars indicate the shot to shot variance at each radial position. Fig.2 shows the density profile determined with the triple probe. The edge density and temperature are in the range $n \simeq 0.5 - 5.0 \times 10^{11}$ cm^{-3}, $T_e \cong$ 5–40 eV and $T_i \cong 2Te$ (Silva, 1989). In the interval $0.87 < r/a < 1.1$ the density scale lenght is $L_n = \left[n / (\frac{dn}{dr})\right] \cong 1.1$ cm whereas the temperature scale lenght is $L_{Te} \cong 1.0$ cm. In the plasma edge the ion Larmor radius was estimated to be $\rho \simeq 0.9$ cm, the ion cyclotron frequency $\Omega_{ci} \cong 6 \times 10^6$ Hz, the electron/ion collision frequency $\nu_{ie} \simeq 1.3 \times 10^5$ s^{-1}.

3. FLUCTUATIONS SPECTRA AND TRANSPORT

Fluctuations profiles were estimated from probe measurements of $\tilde{n}/\langle n\rangle$ and $e\tilde{\varphi}/kT_e$ (space potential was computed from the floating potential) neglecting temperature fluctuations. Root–mean–square fluctuations levels are higher than those observed in other tokamaks. As it can be seen in Fig. 3, $\tilde{n}/\langle n\rangle$ decreases towards the inner regions and $e\tilde{\varphi}/kT_e$ has a maximum near the limiter. The different radial dependence of these variables indicates that the linearized Boltzmann relation $\tilde{n}/n = e\tilde{\varphi}/kT_e$ is not satisfied.

Fig. 4 shows experimental estimation of the $S(k_\theta,\omega)$ poloidal wave–number power spectra, for typical probe measurements of potential and density fluctuations at $r/a = 0{,}87$. The shapes of the poloidal spectra (figs. 4a and 4b) are quite similar and, in both cases, they appear broad and asymmetric about the $k_\theta = 0$ axis, as it has been observed in other tokamaks (Levinson et al., 1984; Holleinstein et al., 1986). The fluctuation power is confined to frequencies $\omega/2\pi < 150$kHz and wave–numbers $|k_\theta| < 3.5$ cm^{-1}. On the other hand, inside the plasma, the toroidal spectrum is broader for density than for the potential fluctuations, which is in contradiction to previous results that showed nearly identical toroidal spectra for $\tilde{n}$ and $\tilde{\varphi}$ (Levinson et al., 1984); however the probes alignment was not accurate to permit definitive conclusions. As usually reported, in this work the poloidal spectra are also broader than the toroidal ones.

Countour plots of the normalized spectrum function $s(k,\omega)$ defined as:

$$s(k,\omega) = \frac{S(k,\omega)}{\sum\limits_{k,\omega} S(k,\omega)} \qquad (1)$$

are shown in Fig.5, for density fluctuations at the positions $r/a=0.87$ ind 1.10. These spectra show a change in the phase velocity. The dominant low wavenumber region is characterized by a broad but peaked poloidal spectrum, the fluctuation power being small

for $k_\theta \geq 3.5\ cm^{-1}$. Similar observations are valid also for potential fluctuations.

Statistical dispersion relations $\bar{k}(\omega)$ and their spectral width $\sigma_k(\omega)$ were computed from the normalized spectra:

$$\bar{k}(\omega) = \sum_k k\, s(k|\omega) \qquad (2)$$

where

$$s(k|\omega) = \frac{s(k,\omega)}{\sum_k s(k,\omega)} \quad ,$$

$$\sigma_k(\omega) = \left[\sum_k k^2 s(k|\omega) - \bar{k}^2(\omega) \right]^{1/2} \quad , \qquad (3)$$

analogous quantities $\bar{\omega}(k)$ and $\sigma_\omega(k)$ were also calculated in terms of wavenumbers.

On the edge plasma the turbulent broadening σ_k and σ_ω have about the same value for the density and potential spectra (typically $\sigma_k \cong 2\ cm^{-1}$ and $\sigma_\omega = 1 \times 10^5 Hz$), but in the scrape–off layer σ_k are higher, and σ_ω are lower, for $\tilde{\varphi}$ than for $\tilde{n}$. Measurements of the correlation lengths resolved in frequency can be obtained by $(\sigma_k)^{-1}$. The correlation time for the $\tilde{\varphi}$ spectra is higher in the scrape–off layer than in the edge plasma, but it does not differ significantly in these regions for the $\tilde{n}$ spectra. The strength of the reported turbulence can be shown by the relative broadenings $\sigma_\omega(k_\theta)/\bar{\omega}(k_\theta) \simeq 1.6$, higher than those obtained in similar experiments in other tokamaks for which the values of this ratio was about one (Levinson et al., 1984; Holleinstein et al., 1986). This stronger turbulence might be caused by poor confinement conditions, typical of small tokamaks.

Power weighted phase velocities v_{ph} in the poloidal direction were obtained from the spectra with:

$$v_{ph} = \sum_{k,\omega} \frac{\omega}{k}\, s(k_\theta,\omega) \quad . \qquad (6)$$

Fig.6 shows the measured v_{ph} radial profile for both $\tilde{\varphi}$ and $\tilde{n}$ fluctuations. As it has been reported (Lin, 1991), the values of v_{ph} are of the same order of magnitude than the diamagnetic drift velocity. In the scrape–off layer, this phase velocity is also comparable to the poloidal rotation velocity E_r/B_ϕ computed from the floating–potential radial profile, but in the plasma edge v_{ph} is almost one order of magnitude smaller than E_r/B_ϕ. The computed phase velocity has the same direction as the ion diamagnetic drift velocity in the edge plasma.

The radial induced particle flux Γ and its spectral distribution $\Gamma(\omega)$, due to electrostatic fluctuations, were estimated from simultaneous measurements of $\tilde{n}$ and $\tilde{\varphi}$ by ensemble averaging over many realizations using (Ritz et al., 1989; Hidalgo et al., 1991; Robinson, 1986):

$$\Gamma = \langle \tilde{n}\, \tilde{v}_r \rangle = 2 \sum_\omega \Gamma(\omega) \qquad (7)$$

with

$$\tilde{v}_r = \tilde{E}_\theta / B_\phi = i k_\theta \tilde{\varphi} / B_\phi \quad . \qquad (8)$$

Fig.7 presents the radial profile of fluctuations induced particle flux with a maximum at the radial location where $\tilde{n}$ and $\tilde{\varphi}$ are maximum. Fig.8 shows typical frequency spectra of poloidal $\tilde{B}_\theta^2$ magnetic fluctuations measured at two different positions. Fig.9 shows typical frequency spectra for $\tilde{B}_\theta$ and $\tilde{B}_r$ at $r/a \cong 1.28$. Radial variation of the normalized fluctuation amplitudes of the poloidal and radial magnetic field ($\dot{\tilde{B}}_\theta/B_\theta(a)$, $\dot{\tilde{B}}r/B_\theta(a)$) estimated from magnetic probe measurements, is shown in Figs.10a and b. Near the wall the decrease of fluctuation amplitude with radius is very pronounced, but there is a significant peak on the $\dot{\tilde{B}}_\theta$ profile at $r/a = 1.24$. This kind of $\dot{\tilde{B}}_\theta$ profiles indicates the existence of low k_θ and ω tearing modes that have been measured also at edge plasmas in

other tokamaks. The spectra of $\tilde{B}_\theta$ and $\tilde{B}_r$ observed in the scrape–off layer are similar for different radial positions except for lower relative level of high–frequency components nearer the wall.

The relationship between the Langmuir and the magnetic probes measurements were investigated by computing the cross–correlation and the coherence between the signals measured by two probes radially separeted from each other by 2.3 cm. An example is shown in Fig.11a, which presents the coherence $\gamma(\omega)$ between $\tilde{n}$ and $\tilde{B}_\theta$ for r/a = 0.99. In this figure the coherence is small, except for ω values near 50kHz that correspond to the peak of the MHD activity observed in the TBR–1 discharges (Vannucci et al., 1989). For the same radial position $\tilde{n}$ and $\tilde{\varphi}$ oscillate almost in phase for frequencies near 25 kHz and, consequently, the transport $\Gamma_{\tilde{n}\tilde{\varphi}}$ is significant only in this frequency range (Fig.12). Moving the probes radially the same effect was not observed behind the limiter and in the scrape–off layer, an indication that the small $\tilde{n}$ and $\tilde{\varphi}$ phase difference for the Mirnov oscillation frequencies could be localized around a resonant magnetic surface. Further investigations under development should give more details about this effect. Thus, in the TBR–1 typical discharges, high MHD activity modulates density and potencial fluctuations at the plasma edge.

4. CONCLUSIONS

Measurements of broadband density, potential, and magnetic fluctuations at the plasma edge presented in this paper illustrate the existence of several distinguishing features under ohmic conditions and high MHD activity, typical of TBR–1 tokamak discharges.

The fluctuations were measured with an appropriate set of Langmuir and magnetic probes, and the density and potential radial profiles were determined by using a triple

probe. The experimental set–up and the correlation technique were based on those used in the TEXT tokamak.

In the analysed discharges $\tilde{\varphi}$ and $\tilde{n}$ are not intrinsically correlated and do not satisfy the linearized Boltzmann relation. The $S(k,\omega)$ poloidal power spectra are poloidally asymmetric and broader than the toroidal ones.

Statistical dispersion relations and their spectral width were computed. In the edge plasma, σ_k and σ_ω have similar values for $\tilde{\varphi}$ and $\tilde{n}$, but in the scrape–off layer σ_k is higher and σ_ω lower for $\tilde{\varphi}$ than $\tilde{n}$. The correlation time for the $\tilde{\varphi}$ spectra is higher in the scrape–off layer than in the edge plasma, but they are approximately the same for the $\tilde{n}$ spectra.

The strength of the turbulence in TBR–1 (given by the relative broadening $\sigma_\omega(k_\theta)/\bar{\omega} \simeq 1.6$) is higher than in other tokamaks. The phase velocity is of the same order than the diamagnetic drift velocities with the same signal of the ion drift velocity in the edge plasma.

The $\tilde{B}_\theta$ and $\tilde{B}_r$ spectra are similar but the radial profiles of their amplitudes are different and seem to be determined by low frequency Mirnov oscillations. Only for these frequencies the correlations between density or potential fluctuations and $\dot{\tilde{B}}_\theta$ or $\dot{\tilde{B}}_r$ are not low.

The particle flux resulting from $\tilde{n}$ and $\tilde{\varphi}$ is outward and was estimated to be of the order of that calculated from Bohn diffusion; it is also limited to frequencies lower than 100 kHz with a peak in the Mirnov oscillations frequency range. At these frequencies $\tilde{n}$ and $\tilde{\varphi}$ oscillations are almost in phase. Turbulence and transport studies in the edge plasma of the TEXT tokamak show that $\tilde{n}$ and $\tilde{\varphi}$ oscillations can be modulated by strong Mirnov oscillations but the transport is small at the Mirnov frequencies and the $\tilde{n}$ and $\tilde{B}_\theta$ spectra superposition is negligible (Lin, 1991). In our results, there is a partial superposition of the $\tilde{B}_\theta$ and $\tilde{n}$ spectra at the Mirnov frequencies and this could influence

the $\tilde{n}\,\tilde{\varphi}$ phase difference at these frequencies and, consequently, increase the transport in this frequency range.

The high MHD activity observed in the analysed discharges creates a stochastic magnetic field in the plasma edge (Lin, 1991) and, as it was suggested recently (Finn et al., 1991), electrostatic sound waves propagation along these stochastic field could contributes to particle field lines transport. This might explain the enhancement of the electrostatic transport at the Mirnov frequencies. There are also evidences that the $\tilde{n}$ and $\tilde{\varphi}$ oscillations, and consequently the electrostatic transport, are modulated by the Mirnov oscillations.

ACKNOWLEDGEMENTS

The authors would like to thank Dr. Hong Lin and Dr. Steve MacCool (Fusion Research Center, The University of Texas at Austin), and Mr. Wanderley P. de Sá (IF–USP) for useful discussions during the development of this work. Several suggestions of Dr. Roger D. Bengtson (Fusion Research Center, The University of Texas at Austin) were very useful to the development of this work.

+ Work partially supported by FAPESP and CNPq.

REFERENCES

Chen S.L., Sekiguchi T. (1965) *J. of Applied Physics* 36, 2363.

Diamond P.H., Drake J.F., Matsumoto H., Sheffield J., Terry P.W., Wootton A.J. (1990) *Comments Plasma Phys. Controlled Fusion* 13, 327.

Duperrex P.A., Hollenstein Ch., Joye B., Keller R., Lister J.B., Marcus F.B., Moret J.M., Pochelon A., Simm W. (1984) *Phys. Lett.* 106A, 133.

Finn J., Guzdar P.N., Chernikov A.A., "Particle Transport and Rotation Damping due to Stochastic Magnetic Field Lines", submitted for publication in Physics of Fluids B.

Hidalgo C., Harris J.H., Uckan T., Bell J.D., Carreras B.A., Dunlop J.L., Dyer G.R., Ritz Ch.P., Wootton A.J., Meier M.A., Rhode T.L., Carter K. (1991) *Nuclear Fusion* **31**, 1471.

Hollenstein Ch., Keller R., Pochelon A., Ryter F., Sawley M.L., Simm W., Weisen H. (1986) Proc. Int. Workshop on Small Scale Turbulence and Anomalous Transport in Magnetized Plasmas (Cargèse, 1986), Editions de Physique, 181.

Karger F., Lackner K. (1977) *Phys. Lett.* A61, 385.

Kim Y.J., Gentle K.W., Ritz Ch.P., Rhodes T.L., Bengtson R.D. (1991) *Phys. of Fluids* **B3**, 674.

Levinson S.J, Beall J.M., Powers E.J., Bengtson R.D. (1984) *Nuclear Fusion* 24, 527.

Lin H. (1991) "Turbulence and Transport Studies in the Edge Plasma of the TEXT Tokamak", Ph.D. dissertation, Report FRCR#401.

Lippman S., Finkenthal M., Moos H.W., McCool S.C., Wootton A.J. (1991) *Nuclear Fusion* 31, 2131.

Powers E.J., "Polyspectral Analysis and its applications". The University of Texas at Austin (1990), to be published.

Ribeiro C., Da Silva R.P., Caldas I.L., TBR–1 Team (1990) 17th European Conference on Controlled Fusion and Plasma Heating (Amsterdam, 1990), I–349.

Ritz Ch.P., Bengtson R.D., Levinson S.J.(1984) Phys. of Fluids 27, 2956.

Ritz Ch.P., Bravenec R.V., Schoch P.M., Bengtson R.D., Boedo J.A., Forster J.C., Gentle K.W., He Y., Hickok R.L., Kim Y.J., Lin H., Phillips P.E., Rhodes T.L., Rowan W.L., Valanju P.M., Wootton J. (1989) *Phys. Rev. Letters* 62, 1844.

Roberts D.E., van Vuuren G.W., Sherwell D., Fletcher J.D., Nothnagel G., Alport M.J., Villiers J.A.M. (1991) 18th European Conference on Controlled Fusion and Physics (Berlin, 1991), I–261.

Robinson D.C. (1986) Proc. Int. Workshop on Small Scale Turbulence and Anomalous Transport in Magnetized Plasmas (Cargèse, 1986), Editions de Physique, 21.

Silva R.P. da (1989) Ph.D. Dissertation, IFUSP, University of São Paulo.

Vannucci A., Nascimento I.C., Caldas I.L. (1989) *Plasma Physics and Controlled Fusion* 31, 147.

Tsui H.Y.W., Wootton A.J.,Schoch P.M. (1991) The University of Texas at Austin, Report FRCR#403.

Wagner F., Becker G., Bchringer K. (1982) *Phys. Rev. Lett.* 49, 1408.

Wootton A.J. (1990) The University of Texas at Austin, Report FRCR#371.

FIGURE CAPTIONS

Fig. 1. Radial profile of temperature (Te) The error bars indicate shot–to–shot variance.

Fig. 2. Radial profile for density, determined with the triple probe.

Fig. 3. Radial dependences of the normalized rms fluctuating amplitudes of potential $e\tilde{\varphi}/kTe$, and density $\tilde{n}/\langle n \rangle$.

Fig. 4. $S(k_\theta,\omega)$ spectra for r = 7.0 cm a) obtained for $\tilde{\varphi}$, b) obtained for $\tilde{n}$.

Fig. 5. Contour plots of the $S(k_\theta,\omega)$ spectra for $\tilde{n}$ a) at $r/a = 0.87$ b) at $r/a = 1.10$.

Fig. 6. Radial dependence of the fluctuation phase velocities a) for $\tilde{\varphi}$ b) for $\tilde{n}$.

Fig. 7. Radial profile of fluctuation induced particle flux Γ .

Fig. 8. Typical frequency spectra of magnetic poloidal fluctuations measured at two different positions.

Fig. 9. Typical frequency spectra for magnetic fluctuations of $\tilde{B}_\theta$ and $\tilde{B}_r$ at $r/a = 1.28$.

Fig. 10. Radial profile of a) normalized magnetic poloidal fluctuations b) normalized radial magnetic fluctuations.

Fig. 11. The relation coherency between poloidal magnetic and density fluctuations. Distance between probes 2.3 cm .

Fig. 12. Particle transport spectrum at $r/a = 0.99$.

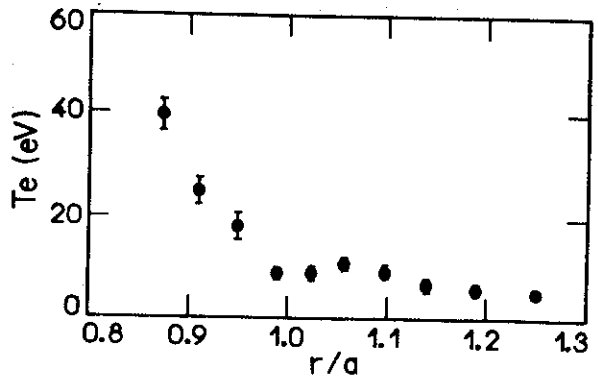

Fig. 1. Radial profile of temperature (Te) The error bars indicate shot–to–shot variance.

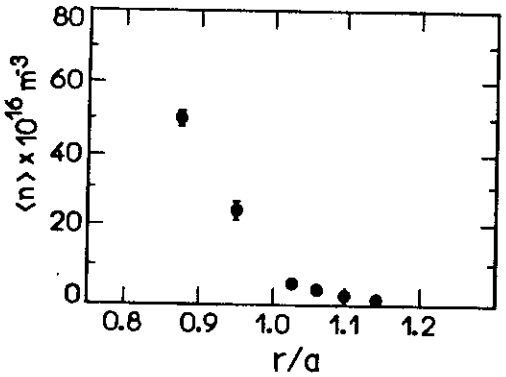

Fig. 2. Radial profile for density, determined with the triple probe.

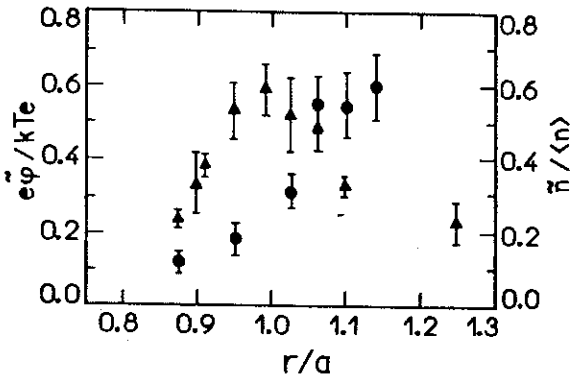

Fig. 3. Radial dependences of the normalized rms fluctuating amplitudes of potential $e\tilde{\varphi}/kTe$, and density $\tilde{n}/\langle n \rangle$.

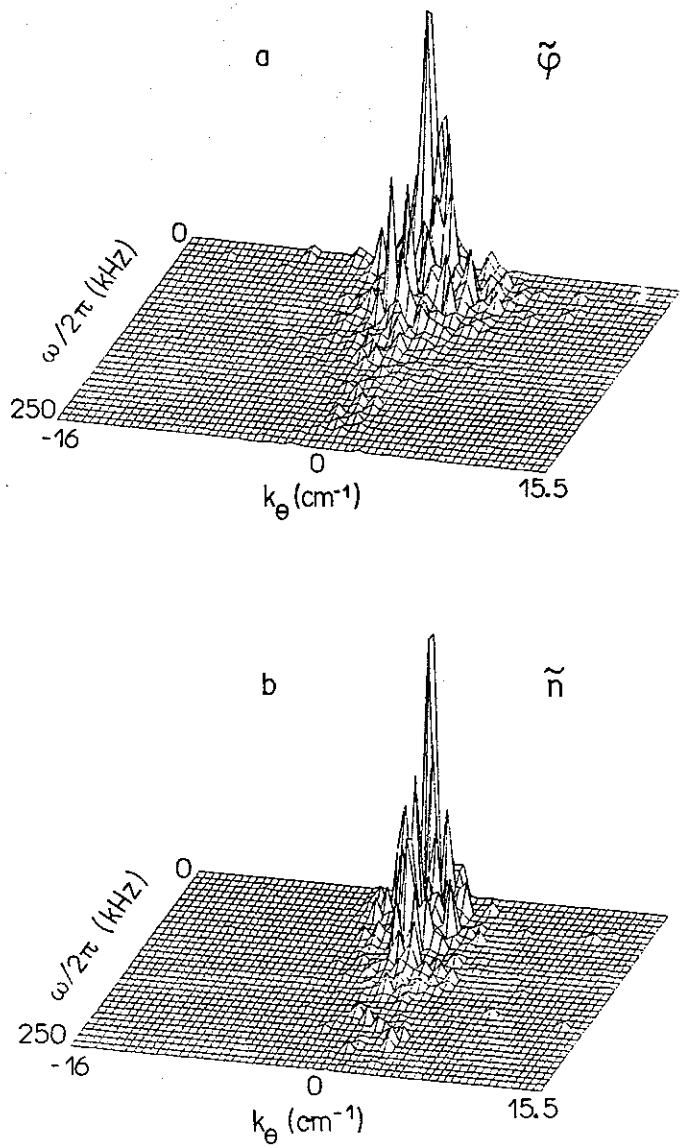

Fig. 4. $S(k_\theta,\omega)$ spectra for r = 7.0 cm a) obtained for $\tilde{\varphi}$, b) obtained for $\tilde{n}$.

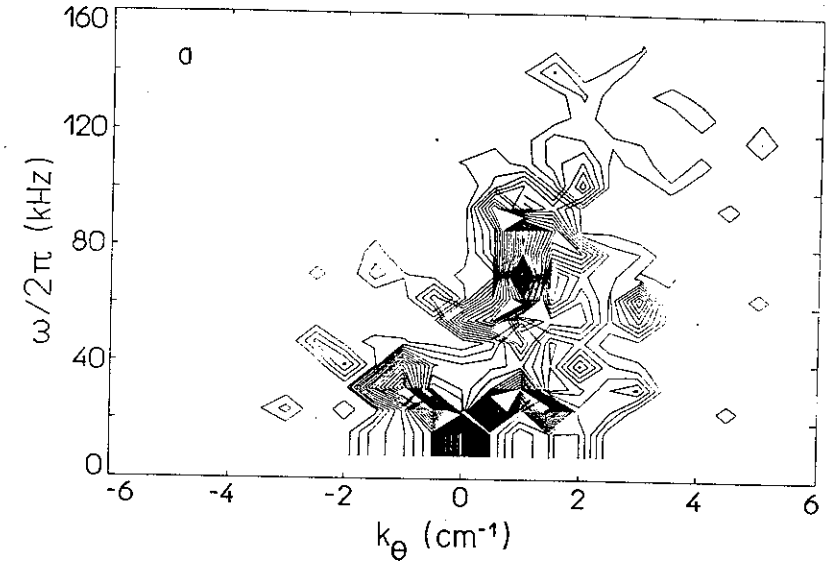

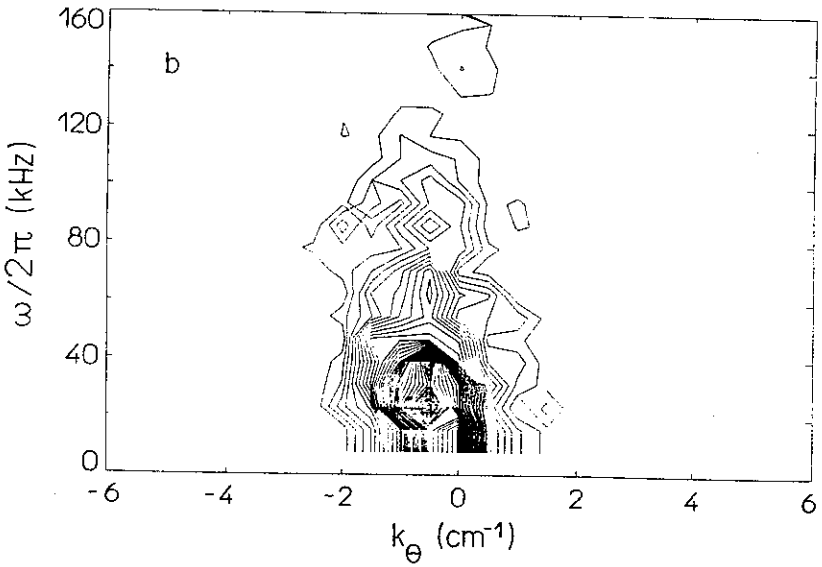

Fig. 5. Contour plots of the $S(k_\theta,\omega)$ spectra for $\tilde{n}$ a) at r/a = 0.87 b) at r/a = 1.10 .

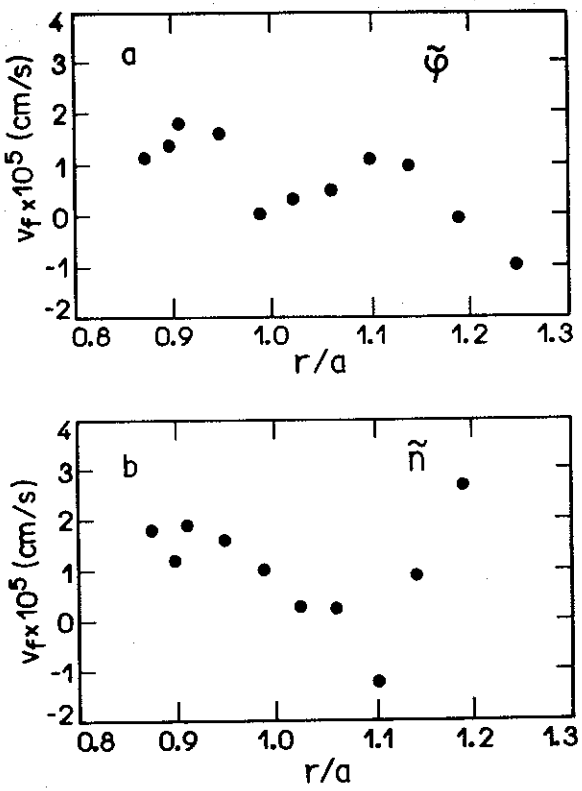

Fig. 6. Radial dependence of the fluctuation phase velocities a) for $\tilde{\varphi}$ b) for $\tilde{n}$.

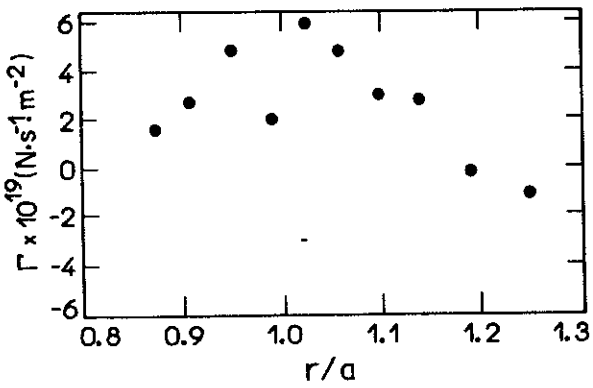

Fig. 7. Radial profile of fluctuation induced particle flux Γ .

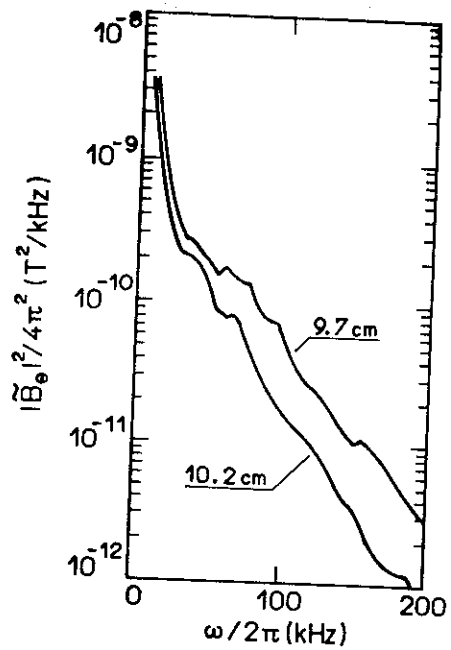

Fig. 8.

Typical frequency spectra of magnetic poloidal fluctuations measured at two different positions.

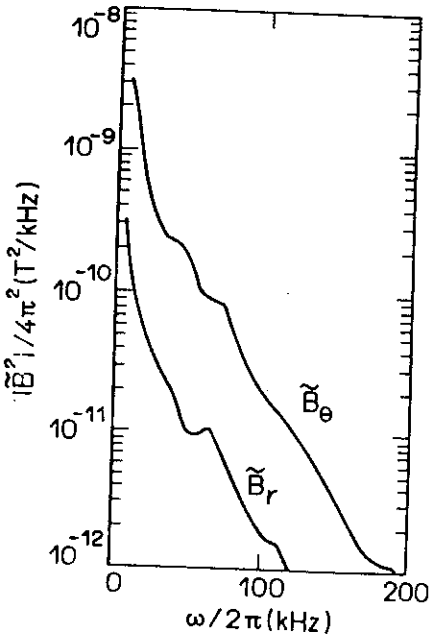

Fig. 9.

Typical frequency spectra for magnetic fluctuations of $\tilde{B}_\theta$ and $\tilde{B}_r$ at r/a = 1.28 .

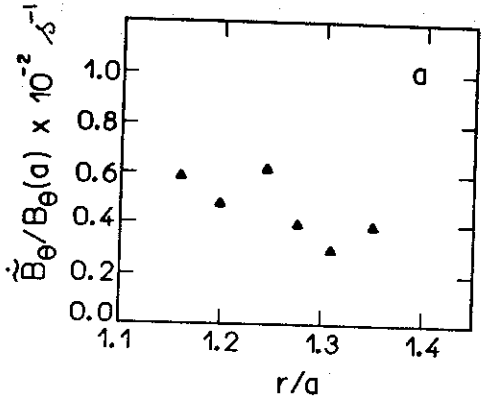

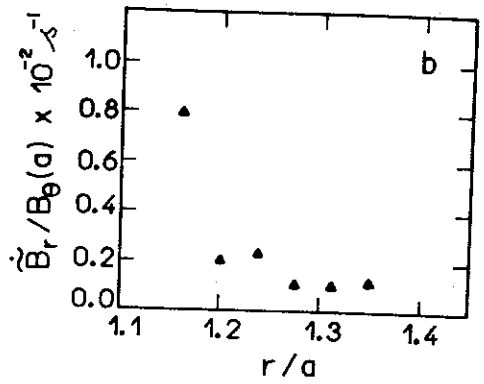

Fig. 10. Radial profile of a) normalized magnetic poloidal fluctuations b) normalized radial magnetic fluctuations.

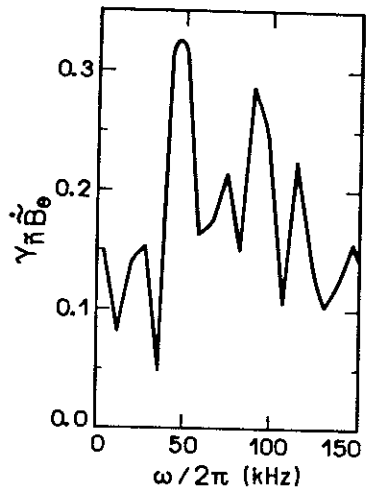

Fig. 11. The relation coherency between poloidal magnetic and density fluctuations. Distance between probes 2.3 cm .

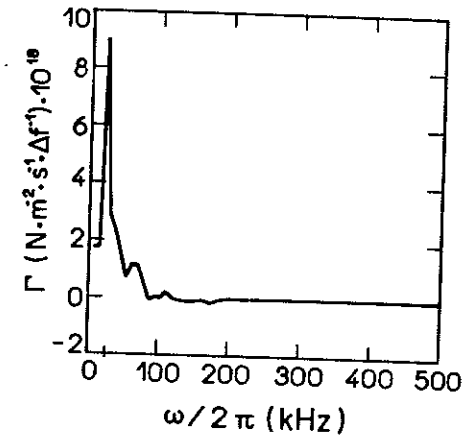

Fig. 12. Particle transport spectrum at r/a = 0.99 .